OPTIMIZED SENSOR SELECTION FOR JOINT RADAR-COMMUNICATION SYSTEMS

Ammar Ahmed, Shuimei Zhang, Yimin D. Zhang

Department of Electrical and Computer Engineering, Temple University, Philadelphia, PA 19122, USA

ABSTRACT

Sensor array-based joint radar-communication (JRC) systems exploit adaptive beamforming to transmit radar and communication signals in their respective directions. Optimal sensor selection is anticipated as an attractive means to achieve superior performance with a low hardware cost because of the ever-decreasing cost of the sensor deployment compared to the radio frequency (RF) chains and processors. In this paper, we address optimal sensor selection for adaptive beamforming-based JRC systems by exploiting a constrained re-weighted ℓ_1-norm minimization with low computational complexity. We argue that, compared to the individual approaches, the grouped counterpart eases the hardware implementation by mollifying the unnecessary sensor switching and enables effective utilization of up-conversion chains. Simulation results clearly demonstrate the superior performance of the proposed strategies.

Index Terms— Adaptive beamforming, joint radar-communication, sensor selection, constrained optimization, spectrum sharing.

1. INTRODUCTION

Spectrum sharing is enjoying a momentous research attention due to the rapidly increasing demand of spectrum resources [1–4]. In this context, great research efforts have been made to enable the co-existence of multiple platforms within the same spectral bands [5–22]. In order to successfully deploy the co-existing radar and communication systems, it is important that both systems cooperate with each other and collaboratively achieve their objectives. This challenge can be significantly simplified if both systems are controlled by a joint control entity. Joint radar-communication (JRC) system is such an example where the radar and communication system objectives are achieved by the same physical platform [4, 6, 8, 9, 12–18].

There are several popular operating configurations of JRC systems. Single transmitter-based JRC systems exploit dual-purpose radar waveforms such that the communication information can be transmitted by waveform selection [1, 2, 17]. Phased array-based JRC systems exhibit an additional feature of spatial multiplexing by utilizing sensor array beamforming to steer dual-purpose waveforms in different directions [4, 6–9, 13–16]. The communication function can be realized either by spatially changing the gain and/or phase of the transmitted waveforms or by employing waveform diversity [4, 9, 12–16]. On the other hand, distributed JRC systems consist of dual-purpose distributed multiple-input multiple-output (MIMO) transducers, which exploit waveform and spatial diversity to carry out both radar and communication operations simultaneously [19].

The focus of this paper is on JRC systems which exploit adaptive beamforming to perform both radar and communication tasks. An example of such a system is shown in Fig. 1. In order to improve the system performance with a low complexity, there is a trend to use a high number of sensors, whereas keeping a very low number of hardware up-conversion chains and processors. Great research efforts have been invested in the direction of antenna selection and combining for various communications and radar applications [19, 23–28]. For JRC systems, these efforts focus on the optimal sensor selection in distributed [19] as well as colocated sensor array-based systems [26, 28].

In this paper, we present a novel sensor selection strategy for sensor array-based JRC system. The objective is to select the minimum number of sensors while ensuring the desired radar and communications operation requirements. We formulate a convex optimization problem which addresses this objective in two different ways. In the first approach, we optimize the array geometry for each beamformer to satisfy a certain set of joint radar and communication objectives. To avoid frequent sensor switching in slow time required by this approach, our second approach optimizes the array geometry by jointly considering all beamformers and subsequently mollifies the complexity of hardware implementation.

Notations: Lower-case (upper-case) bold characters are used to denote vectors (matrices). $(\cdot)^*$, $(\cdot)^{\mathrm{T}}$ and $(\cdot)^{\mathrm{H}}$ represent the conjugate, transpose and the Hermitian transpose operators, respectively. $|\cdot|$, $\|\cdot\|_0$, $\|\cdot\|_1$, and $\|\cdot\|_2$ respectively denote the absolute value, ℓ_0-, ℓ_1- and ℓ_2-norms. Moreover, $\mathbf{1}_{M\times 1}$ denotes the M-length column vector of all ones whereas $\odot$ represents the element-wise product operation.

2. SIGNAL MODEL OF JRC SYSTEM

Consider a JRC system consisting of an M-element transmit linear array. The JRC system exploits different beamforming weight vectors over time to transmit communication information towards the communication receivers such that all beamforming vectors offer similar radar mainlobe profile. The vector $\mathbf{a}(\theta) = [e^{j2\pi d_1 \sin(\theta)/\lambda}, \ldots, e^{j2\pi d_M \sin(\theta)/\lambda}]^{\mathrm{T}}$ represents the array manifold where d_m is the location of the mth sensor

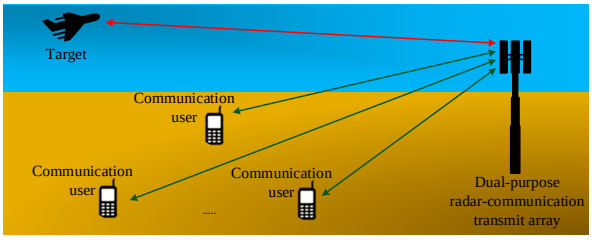

Fig. 1. Joint radar-communication system.

$(1 \leq m \leq M)$ and λ is the signal wavelength. The radar surveillance region, sidelobe region, and the transition region are respectively denoted by Θ_{rad}, Θ_{sl}, and Θ_{trans}. We consider C communication users located within the sidelobe region of the radar, and the angular direction of the cth user $(1 \leq c \leq C)$ is θ_c, where $\theta_c \in \Theta_{\text{com}} \subset \Theta_{\text{sl}}$. The JRC system exploits N beamforming weight vectors where the vector $\mathbf{u}_n$ $(1 \leq n \leq N)$ satisfying the radar and communication objectives can be obtained from the following optimization [16]:

$$\begin{aligned} &\min_{\mathbf{u}_n} \max_{\theta_r} \left| G_{\text{rad}} e^{j\varphi(\theta_r)} - \mathbf{u}_n^{\text{H}} \mathbf{a}(\theta_r) \right|, && \theta_r \in \Theta_{\text{rad}}, \\ &\text{subject to } \left| \mathbf{u}_n^{\text{H}} \mathbf{a}(\theta_\varepsilon) \right| \leq \varepsilon_{\text{sl}}, && \theta_\varepsilon \in \Theta_{\text{sl}}, \\ &\qquad \mathbf{u}_n^{\text{H}} \mathbf{a}(\theta_c) = e^{j\phi_{n,c}} \Delta_{n,c}, && 1 \leq c \leq C, \end{aligned} \tag{1}$$

where G_{rad} is the desired array gain in the mainlobe region, $\varphi(\cdot)$ denotes the desired phase profile, and ε_{sl} is the maximum allowable sidelobe amplitude level. The distinct gain and phase associated with the direction of communication user c, respectively denoted as $\Delta_{n,c}$ and $e^{j\phi_{n,c}}$, represent the transmitted communication information towards that user. Note that this scheme enables multiple access by using distinct amplitudes and phases, as embedded in a QAM symbol, towards different communication receivers [16]. Note that, in order to use L amplitudes and Q phases towards each communication receiver, the JRC system requires $N = (LQ)^C$ unique beamforming weight vectors.

The JRC system exploits K dual-purpose waveforms which are utilized for both radar and communication operations. These waveforms $\psi_1(t), \psi_2(t), \ldots, \psi_K(t)$ satisfy the following orthogonality property:

$$\frac{1}{T} \int_0^T \psi_{k_1}(t) \, \psi_{k_2}^*(\tau) \mathrm{d}t = \delta(k_1 - k_2) \, \delta(t - \tau), \tag{2}$$

where $1 \leq k_1, k_2 \leq K$ are positive integers, t is the fast time, T denotes the time duration of each radar pulse, $\psi_{k_2}(\tau)$ represents the time-delayed version of $\psi_{k_2}(t)$ delayed by time $\tau - t$ $(< T)$, and $\delta(\cdot)$ is the Kronecker delta function.

For the nth beamforming vector, the transmit signal from the JRC sensor array takes the following form:

$$\mathbf{x}(t) = \mathbf{u}_n \psi_k(t), \tag{3}$$

where the beamforming vector $\mathbf{u}_n$ satisfies the radar mainlobe gain objective and projects the QAM symbols with amplitude $\Delta_{n,c}$ and phase $e^{j\phi_{n,c}}$ towards the cth communication user

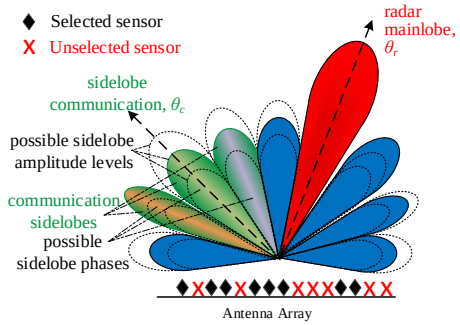

Fig. 2. Sensor selection for JRC system ('x' denotes unselected sensor positions).

exploiting waveform $\psi_k(t)$. The JRC system can vary the transmitted communication information by exploiting different beamforming weight vectors and the corresponding waveforms over the course of slow time [16].

3. SENSOR SELECTION STRATEGIES

We propose two sensor selection strategies for transmit beamforming-based JRC system. In both cases, the JRC system optimizes the beamforming weight vectors such that the number of selected sensors and the transmit power is minimized. Since these two objectives may be conflicting, more emphasis is given to the sensor selection objective. The main idea of JRC system with sensor selection is illustrated in Fig. 2.

In the first scheme, the sensors are separately selected for each individual beamforming weight vector. Although this scheme works well in theory, it renders frequent sensor switching when different beamforming weight vectors are associated with different sensor selection patterns, resulting in unnecessary implementation complexity for such a system. In addition, this generally requires more sensors, as the union of the selected sensor patterns for all beamformers, to be activated. In the second scheme, we present a joint sensor selection strategy while extracting multiple beamforming weight vectors concurrently. As such, the latter approach avoids sensor switching, leading to a simpler and more practical hardware implementation. Since all beamformers exploit the same set of selected sensors in this strategy, it results in effective sensor utilization compared to the first strategy. The details of these two approaches are respectively discussed in the following two subsections.

3.1. Sensor Selection for Individual Beamformers

We minimize the total number of active sensors as well as the total transmit power of the JRC system through the following multi-objective optimization:

$$\begin{aligned} &\min_{\mathbf{u}_n} \ \|\mathbf{u}_n\|_2^2 + \eta \|\mathbf{u}_n\|_0 \\ &\text{s.t.} \ \ |G_{\text{rad}} e^{j\varphi(\theta_r)} - \mathbf{u}_n^{\text{H}} \mathbf{a}(\theta_r)| \leq \gamma_{\text{tol}}, && \theta_r \in \Theta_{\text{rad}}, \\ &\qquad |\mathbf{u}_n^{\text{H}} \mathbf{a}(\theta_\varepsilon)| \leq \varepsilon_{\text{sl}}, && \theta_{\text{sl}} \in \Theta_{\text{sl}}, \\ &\qquad \mathbf{u}_n^{\text{H}} \mathbf{a}(\theta_c) = \Delta_{n,c} e^{j\phi_{n,c}}, && c = 1, \cdots, C. \end{aligned} \tag{4}$$

Here, η is the tuning parameter which trades off between the two objectives, and γ_{tol} is the maximum bearable tolerance for the radar mainlobe. The ℓ_0-norm-based non-convex objective tries to minimize the number of selected sensors and ℓ_2-norm-based objective tends to minimize the total transmit power. The ℓ_0-norm in (4) can be relaxed by exploiting the ℓ_1-norm, albeit a weaker and indirect measure of sparsity [29], resulting in the following optimization:

$$\begin{aligned} \min_{\mathbf{u}_n} \quad & \|\mathbf{u}_n\|_2^2 + \eta \|\mathbf{u}_n\|_1 \\ \text{s.t.} \quad & |G_{\text{rad}} e^{j\varphi(\theta_r)} - \mathbf{u}_n^{\text{H}} \mathbf{a}(\theta_r)| \leq \gamma_{\text{tol}}, \quad \theta_r \in \Theta_{\text{rad}}, \\ & |\mathbf{u}_n^{\text{H}} \mathbf{a}(\theta_\varepsilon)| \leq \varepsilon_{\text{sl}}, \qquad \theta_{\text{sl}} \in \Theta_{\text{sl}}, \\ & \mathbf{u}_n^{\text{H}} \mathbf{a}(\theta_c) = \Delta_{n,c} e^{j\phi_{n,c}}, \qquad c = 1, \cdots, C. \end{aligned} \tag{5}$$

While Eq. (5) enforces sparsity in the beamforming weight vector $\mathbf{u}_n$ by exploiting the ℓ_1-norm, the sensors with a higher beamforming gain are penalized more compared to those with a lower beamforming gain, thus yielding a suboptimal sparsity solution. This issue can be mitigated by introducing a reweighting function in the ℓ_1-norm-based objective function (5) to enforce the sparsity in a democratic way as follows:

$$\begin{aligned} \min_{\mathbf{u}_n} \quad & \|\mathbf{u}_n\|_2^2 + \eta \left\| \mathbf{w}_n^{(i)} \odot \mathbf{u}_n \right\|_1 \\ \text{s.t.} \quad & |G_{\text{rad}} e^{j\varphi(\theta_r)} - \mathbf{u}_n^{\text{H}} \mathbf{a}(\theta_r)| \leq \gamma_{\text{tol}}, \quad \theta_r \in \Theta_{\text{rad}}, \\ & |\mathbf{u}_n^{\text{H}} \mathbf{a}(\theta_\varepsilon)| \leq \varepsilon_{\text{sl}}, \qquad \theta_{\text{sl}} \in \Theta_{\text{sl}}, \\ & \mathbf{u}_n^{\text{H}} \mathbf{a}(\theta_c) = \Delta_{n,c} e^{j\phi_{n,c}}, \qquad c = 1, \cdots, C, \end{aligned} \tag{6}$$

where superscript (i) denotes the ith iteration. The mth element of the weighting function $\mathbf{w}_n$ is expressed as [29]:

$$w_{n,m} = \begin{cases} \dfrac{1}{|u_{n,m}|}, & \text{if } |u_{n,m}| > 0, \\ 1/\zeta, & \text{if } |u_{n,m}| = 0, \end{cases} \tag{7}$$

where $u_{n,m}$ is the mth element of $\mathbf{u}_n$, and ζ should be set slightly smaller than the expected nonzero magnitudes of $\mathbf{u}_n$. The optimization (6) is executed in an iterative manner such that the coefficients $\mathbf{w}_n^{(i+1)}$ are updated using the beamforming weights $\mathbf{u}_n$ after the ith iteration. For the first iteration, $\mathbf{w}_n^{(1)} = \mathbf{1}_{M\times 1}$. The solution of such iterative ℓ_1-norm-based optimization is closer to the ℓ_0-norm-based counterpart within few (e.g., 2 to 15) iterations [29].

3.2. Group Sparsity-based Joint Sensor Selection for Multiple Beamformers

As we discussed above, the optimization (6) for different individual beamforming weight vectors may result in different sets of selected sensors. This is highly undesirable because the required frequent sensor switching introduces unnecessary complexity in hardware implementation. Moreover, all the beamforming weight vectors collectively use a higher number of sensors even though each individual beamforming weight vector exploits very few sensors.

We propose a joint optimal sensor selection strategy which minimizes the total number of sensors used by all the beamformers for the JRC operation. For this purpose, we exploit the mixed $\ell_{1,2}$-norm-based group-sparsity concept [30]. The mixed $\ell_{1,2}$-norm is defined as:

$$\|\mathbf{u}\|_{1,2} = \sum_{m=1}^{M} \left(\sum_{n=1}^{N} |u_{n,m}|^2 \right)^{1/2}. \tag{8}$$

The proposed multi-objective optimization for sensor selection exploits group-sparsity to extract all beamforming weight vectors and takes the following form:

$$\begin{aligned} \min_{\mathbf{u}_n} \quad & \sum_{n=1}^{N} \|\mathbf{u}_n\|_2^2 + \eta \|\mathbf{u}\|_{1,2} \\ \text{s.t.} \quad & |G_{\text{rad}} e^{j\varphi(\theta_r)} - \mathbf{u}_n^{\text{H}} \mathbf{a}(\theta_r)| \leq \gamma_{\text{tol}}, \quad \theta_r \in \Theta_{\text{rad}}, \\ & |\mathbf{u}_n^{\text{H}} \mathbf{a}(\theta_\varepsilon)| \leq \varepsilon_{\text{sl}}, \qquad \theta_{\text{sl}} \in \Theta_{\text{sl}}, \\ & \mathbf{u}_n^{\text{H}} \mathbf{a}(\theta_c) = \Delta_{n,c} e^{j\phi_{n,c}}, \qquad c = 1, \cdots, C. \end{aligned} \tag{9}$$

Note that, contrary to the optimization (6) which is exploited for each beamforming weight vector separately, the optimization (9) jointly solves all N beamforming vectors simultaneously. The mixed $\ell_{1,2}$-norm enforces the group sparsity, resulting in the selection of exactly the same sensors for all the beamforming weight vectors. However, each beamforming weight vector will have unique weights depending on its radar and communication requirements.

Similar to the weighting function in Eq. (7), the group sparsity in optimization (9) can also be enhanced democratically by exploiting a similar weighting function as follows:

$$v_m = \begin{cases} \left(\sum_{n=1}^{N} |u_{n,m}|^2 \right)^{-1/2}, & \text{if } \sum_{n=1}^{N} |u_{n,m}|^2 > 0, \\ 1/\zeta, & \text{if } \sum_{n=1}^{N} |u_{n,m}|^2 = 0, \end{cases} \tag{10}$$

where v_m denotes the weight for the mth sensor. The resulting group sparsity-based optimization jointly produces all N beamforming weight vectors as:

$$\begin{aligned} \min_{\mathbf{u}_n} \quad & \sum_{n=1}^{N} \|\mathbf{u}_n\|_2^2 + \eta \left\| \mathbf{v}^{(i)} \odot \mathbf{u} \right\|_{1,2} \\ \text{s.t.} \quad & |G_{\text{rad}} e^{j\varphi(\theta_r)} - \mathbf{u}_n^{\text{H}} \mathbf{a}(\theta_r)| \leq \gamma_{\text{tol}}, \quad \theta_r \in \Theta_{\text{rad}}, \\ & |\mathbf{u}_n^{\text{H}} \mathbf{a}(\theta_\varepsilon)| \leq \varepsilon_{\text{sl}}, \qquad \theta_{\text{sl}} \in \Theta_{\text{sl}}, \\ & \mathbf{u}_n^{\text{H}} \mathbf{a}(\theta_c) = \Delta_{n,c} e^{j\phi_{n,c}}, \qquad c = 1, \cdots, C, \end{aligned} \tag{11}$$

where $\mathbf{v}^{(i)}$ denotes the weighting function obtained in the ith iteration and

$$\|\mathbf{v} \odot \mathbf{u}\|_{1,2} = \sum_{m=1}^{M} \left(\sum_{n=1}^{N} |v_m u_{n,m}|^2 \right)^{1/2} = \sum_{m=1}^{M} v_m \left(\sum_{n=1}^{N} |u_{n,m}|^2 \right)^{1/2}. \tag{12}$$

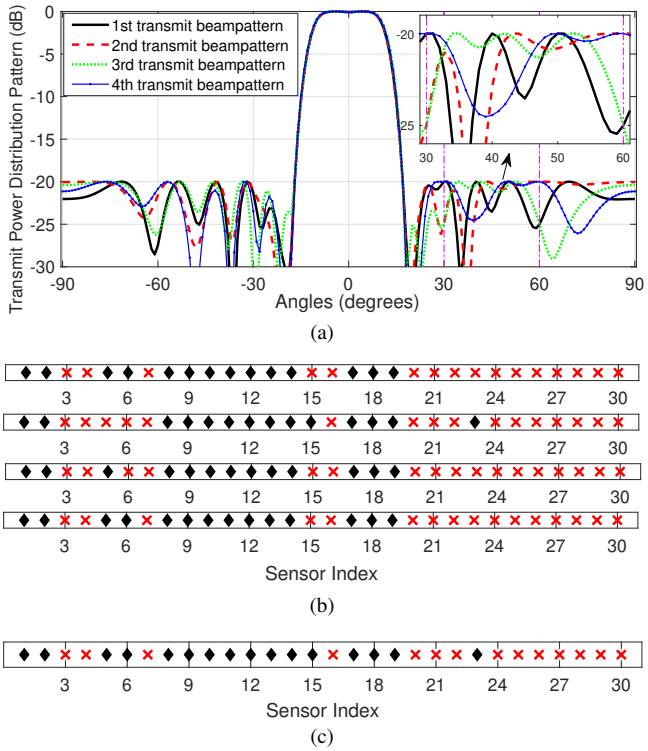

Fig. 3. Sensor selection for the first strategy: (a) Transmit power pattern, (b) Final sensor selection profile for each beampattern, (c) Overall sensor selection profile containing sensors selected by all beamforming weight vectors.

Eq. (11) is solved in an iterative fashion until the convergence is achieved. This multi-objective optimization tends to select the array sensors that are shared by all beamforming weight vectors and minimizes the total transmit power.

4. SIMULATION RESULTS

In all simulations, we consider a uniform linear array (ULA) consisting of $M = 30$ transmit sensors separated by 0.5λ. In addition to the radar with a mainbeam of 0 dB gain between -7^{o} and 7^{o}, the array serves for two ($C = 2$) communication users located in the sidelobe region at angles 30^{o} and 60^{o}, respectively. The maximum allowable sidelobe level ε_{sl} is set to -20 dB. For the convenience of illustrating the transmit beampatterns, we consider BPSK signaling where the JRC transmit array has an objective to transmit two different amplitude levels of -20 dB and -25 dB towards both communication receivers, resulting in four distinct beamforming weight vectors. The tuning coefficient η is set to unity for all multi-objective optimization problems.

For the first strategy, we individually synthesized the four beamforming weight vectors through (6), and the beampatterns are illustrated in Fig. 3(a). The final sensor selection profile for these respective beamformers is shown in Fig. 3(b). It is observed that these beamforming weight vectors respectively use 14, 14, 13, and 14 sensors. As a result, overall 16 sensors are needed, as depicted in Fig. 3(c). For large number of beamforming vectors, such difference in the selected sensors corresponding to each beamforming vector will require a high number of sensors, thus inviting frequent sensor switching, a high hardware complexity, and suboptimal sensor utilization.

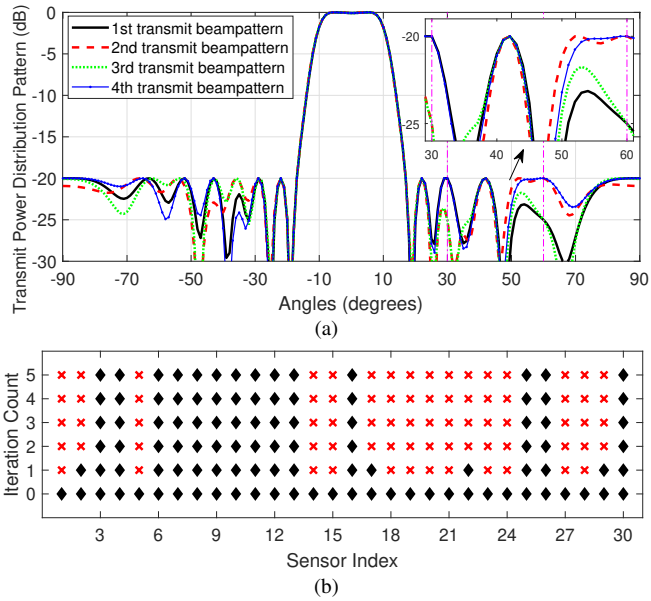

Fig. 4. Group sparsity-based joint sensor selection for all beamforming weight vectors: (a) Transmit power pattern, (b) Spatial sensor selection profile with respect to iteration count.

For the second strategy, the group sparsity-based sensor selection for all the beamforming weight vectors is achieved through (11). The same parameters are used. Fig. 4(a) shows that the radar and communication performance remains the same as compared to the first strategy as shown in Fig. 3(a). However, Fig. 4(b) shows that only 14 sensors are used by this approach, which is less than the total number of 16 sensors used in Fig. 3(c). Moreover, it is noted that the re-weighted iterative algorithm converges very fast (2 to 10 iterations for all the simulations).

5. CONCLUSION

We presented two novel sensor selection strategies for the JRC system based on the extraction of individual and grouped beamforming weight vectors, respectively. The proposed strategies rely on multi-objective optimization which aims to select the lowest number of sensors and minimize the overall power consumption. The group sparsity-based strategy is more useful and effective as it renders less total number of sensors and avoids frequent sensor switching, thus enabling effective utilization of RF chains and easing hardware implementations.

REFERENCES

[1] C. Sturm, T. Zwick, and W. Wiesbeck, "An OFDM system concept for joint radar and communications operations," in *Proc. IEEE Veh. Technol. Conf.*, Barcelona, Spain, Apr. 2009.

[2] S. D. Blunt, M. R. Cook, and J. Stiles, "Embedding information into radar emissions via waveform implementation," in *Proc. Waveform Diversity and Design Conf.*, Niagara Falls, Canada, Aug. 2010, pp. 195–199.

[3] H. Griffiths, S. Blunt, L. Cohen, and L. Savy, "Challenge problems in spectrum engineering and waveform diversity," in *Proc. IEEE Radar Conf.*, Ottawa, Canada, Apr.–May 2013, pp. 1–5.

[4] A. Hassanien, M. G. Amin, Y. D. Zhang, and F. Ahmad, "Signaling strategies for dual-function radar communications: An overview," *IEEE Aerosp. Electron. Syst. Mag.*, vol. 31, no. 10, pp. 36–45, Oct. 2016.

[5] D. W. Bliss, "Cooperative radar and communications signaling: The estimation and information theory odd couple," in *Proc. IEEE Radar Conf.*, Cincinnati, OH, May 2014, pp. 50–55.

[6] J. Euzière, R. Guinvarc'h, M. Lesturgie, B. Uguen, and R. Gillard, "Dual function radar communication time-modulated array," in *Proc. Int. Radar Conf.*, Lille, France, Oct. 2014, pp. 1–4.

[7] Z. Geng, H. Deng, and B. Himed, "Adaptive radar beamforming for interference mitigation in radar-wireless spectrum sharing," *IEEE Signal Process. Lett.*, vol. 22, no. 4, pp. 484–488, Apr. 2015.

[8] J. R. Guerci, R. M. Guerci, A. Lackpour, and D. Moskowitz, "Joint design and operation of shared spectrum access for radar and communications," in *Proc. IEEE Radar Conf.*, Arlington, VA, May 2015, pp. 761–766.

[9] A. Hassanien, M. G. Amin, Y. D. Zhang, and F. Ahmad, "Dual-function radar-communications: Information embedding using sidelobe control and waveform diversity," *IEEE Trans. Signal Process.*, vol. 64, no. 8, pp. 2168–2181, Apr. 2016.

[10] A. Hassanien, M. G. Amin, Y. D. Zhang, and F. Ahmad, "Dual-function radar-communications using phase-rotational invariance," in *Proc. European Signal Process. Conf.*, Nice, France, Aug.-Sept. 2015.

[11] S. Zhang, Y. Gu, B. Wang, and Y. D. Zhang, "Robust astronomical imaging under coexistence with wireless communications," in *Proc. Asilomar Conf. Signals, Systems, and Computers*, Pacific Grove, CA, Oct. 2017, pp. 1301–1305.

[12] Y. Liu, G. Liao, J. Xu, Z. Yang, and Y. Zhang, "Adaptive OFDM integrated radar and communications waveform design based on information theory," *IEEE Commun. Lett.*, vol. 21, no. 10, pp. 2174–2177, Oct. 2017.

[13] A. Ahmed, Y. D. Zhang, and B. Himed, "Multi-user dual-function radar-communications exploiting sidelobe control and waveform diversity," in *Proc. IEEE Radar Conf.*, Oklahoma City, OK, Apr. 2018.

[14] F. Liu, L. Zhou, C. Masouros, A. Li, W. Luo, and A. Petropulu, "Toward dual-functional radar-communication systems: Optimal waveform design," *IEEE Trans. Signal Process.*, vol. 66, no. 16, pp. 4264–4279, Aug. 2018.

[15] A. Ahmed, Y. Gu, D. Silage, and Y. D. Zhang, "Power-efficient multi-user dual-function radar-communication," in *Proc. IEEE Int. Workshop Signal Process. Advances in Wireless Commun.*, Kalamata, Greece, June 2018, pp. 1–5.

[16] A. Ahmed, Y. D. Zhang, and Y. Gu, "Dual-function radar-communications using QAM-based sidelobe modulation," *Digital Signal Process.*, vol. 82, pp. 166–174, Nov. 2018.

[17] M. Bică and V. Koivunen, "Radar waveform optimization for target parameter estimation in cooperative radar-communications systems," *IEEE Trans. Aerosp. Electron. Syst.*, vol. 55, no. 5, pp. 2314–2326, Oct. 2019.

[18] M. Bică and V. Koivunen, "Multicarrier radar-communications waveform design for RF convergence and coexistence," in *Proc. IEEE Int. Conf. Acoust., Speech, Signal Process.*, Brighton, U.K., May 2019, pp. 7780–7784.

[19] A. Ahmed, Y. D. Zhang, and B. Himed, "Distributed dual-function radar-communication MIMO system with optimized resource allocation," in *Proc. IEEE Radar Conf.*, Boston, MA, Apr. 2019.

[20] S. Zhang, Y. Gu, and Y. D. Zhang, "Robust astronomical imaging in the presence of radio frequency interference," *J. Astronom. Instrument.*, vol. 8, no. 1, pp. 1–15, 2019.

[21] A. Ahmed, Y. D. Zhang, A. Hassanien, and B. Himed, "OFDM-based joint radar-communication system: Optimal sub-carrier allocation and power distribution by exploiting mutual information," in *Proc. Asilomar Conf. Signals, Systems, and Computers*, Pacific Grove, CA, Nov. 2019.

[22] A. Ahmed, S. Zhang, V. S. Amin, and Y. D. Zhang, "Spectrum sharing strategy for radio frequency based medical services," in *Proc. IEEE Signal Process. in Medicine and Biology Symp.*, Philadelphia, PA, Dec. 2019.

[23] O. Mehanna, N. D. Sidiropoulos, and G. B. Giannakis, "Joint multicast beamforming and antenna selection," *IEEE Trans. Signal Process.*, vol. 61, no. 10, pp. 2660–2674, May 2013.

[24] G. Venkatraman, A. Tölli, M. Juntti, and L. Tran, "Multigroup multicast beamformer design for MISO-OFDM with antenna selection," *IEEE Trans. Signal Process.*, vol. 65, no. 22, pp. 5832–5847, Nov 2017.

[25] O. Tervo, L. Tran, H. Pennanen, S. Chatzinotas, B. Ottersten, and M. Juntti, "Energy-efficient multicell multigroup multicasting with joint beamforming and antenna selection," *IEEE Trans. Signal Process.*, vol. 66, no. 18, pp. 4904–4919, Sep. 2018.

[26] X. Wang, A. Hassanien, and M. G. Amin, "Sparse transmit array design for dual-function radar communications by antenna selection," *Digital Signal Process.*, vol. 83, pp. 223–234, Dec. 2018.

[27] M. Guo, Y. D. Zhang, and T. Chen, "DOA estimation using compressed sparse array," *IEEE Trans. Signal Process.*, vol. 66, no. 15, pp. 4133–4146, Aug. 2018.

[28] X. Wang, A. Hassanien, and M. G. Amin, "Dual-function MIMO radar communications system design via sparse array optimization," *IEEE Trans. Aerosp. Electron. Syst.*, vol. 55, no. 3, pp. 1213–1226, June 2019.

[29] E. J. Candès, M. B. Wakin, and S. P. Boyd, "Enhancing sparsity by reweighted ℓ_1 minimization," *J. Fourier Anal. Appl.*, vol. 14, no. 5, pp. 877–905, Dec. 2008.

[30] M. Yuan and Y. Lin, "Model selection and estimation in regression with grouped variables," *J. R. Stat. Soc. B.*, vol. 68, pp. 49–67, Feb. 2006.